Cell differentiation modeled via a coupled two-switch regulatory network

D. Schittler,[a] J. Hasenauer, F. Allgöwer, and S. Waldherr
Institute for Systems Theory and Automatic Control, University of Stuttgart, 70550 Stuttgart, Germany

(Received 29 July 2010; accepted 4 October 2010; published online 30 December 2010)

Mesenchymal stem cells can give rise to bone and other tissue cells, but their differentiation still escapes full control. In this paper we address this issue by mathematical modeling. We present a model for a genetic switch determining the cell fate of progenitor cells which can differentiate into osteoblasts (bone cells) or chondrocytes (cartilage cells). The model consists of two switch mechanisms and reproduces the experimentally observed three stable equilibrium states: a progenitor, an osteogenic, and a chondrogenic state. Conventionally, the loss of an intermediate (progenitor) state and the entailed attraction to one of two opposite (differentiated) states is modeled as a result of changing parameters. In our model in contrast, we achieve this by distributing the differentiation process to two functional switch parts acting in concert: one triggering differentiation and the other determining cell fate. Via stability and bifurcation analysis, we investigate the effects of biochemical stimuli associated with different system inputs. We employ our model to generate differentiation scenarios on the single cell as well as on the cell population level. The single cell scenarios allow to reconstruct the switching upon extrinsic signals, whereas the cell population scenarios provide a framework to identify the impact of intrinsic properties and the limiting factors for successful differentiation. © *2010 American Institute of Physics*. [doi:10.1063/1.3505000]

Stem cells and their ability to give rise to multiple cell types have become a major topic in systems biology and mathematical modeling.[1–7] This paper presents a mathematical model of functional mechanisms guiding the differentiation of progenitor cells into bone or cartilage cells. We introduce a generic model combining two switch parts: unspecific differentiation stimuli operate on one part of the switch, enabling the cell system to leave the progenitor state, whereas lineage-specific stimuli act on the other part of the switch, determining which of the differentiated cell types will be adopted. To achieve the ultimate goal of guiding stem cells toward cell tissue such as bone transplants, it will be crucial to detect limiting factors and design optimal stimulus conditions. With our model, we demonstrate how, e.g., applying the stimulus components in a certain sequence might improve the differentiation success rate.

I. INTRODUCTION

In recent years, understanding cell differentiation has gained wide interest. Stem cells promise to offer a high potential for medical therapies and tissue engineering due to their multipotency. Mesenchymal stem cells (MSCs) are a particular type of stem cells that can be derived from adults and can give rise to various types of tissue such as bone and cartilage.[8] Therefore, special interest concerns their targeted application for bone or cartilage transplants. However, scientists are far from a detailed knowledge of the processes governing cell fate commitment, differentiation, and maintenance of completely differentiated cell types.

Commonly, cell differentiation is viewed as a process of subsequent decisions; at each decision point, a genetic switch determines which of the possible cell fates is adopted. This view has been formulated in a mathematical modeling framework[5] in terms of binary switch modules. During recent years, systems biology and models of cell differentiation have greatly improved the understanding of certain types of stem cells such as hematopoietic stem cells.[1–4] For other types such as MSCs, however, the key determinants guiding differentiation are still poorly known. There is, to our knowledge, only one mathematical model including MSC lineages, embedded in a more general model of competing lineages.[7] In our model instead, we focus on a subset of lineages for one decision step. This allows us to extend the bifurcation analysis to separate inputs, and to apply these inputs in various orders. Contrary to the modeling of metabolic networks, which can often benefit from more quantitative knowledge of biochemical reactions, modeling of gene regulation struggles with the complexity but yet sparse knowledge of involved processes. Thus, dynamical models of gene regulation usually simplify and reduce to a low number of key regulators and their functional relationships.[1–3]

A common way to qualitatively model cell differentiation is by the widespread minimal motif of two genes or transcriptional regulators (TRs) with mutual inhibition.[1–3,5,9] Such a genetic switch can have several equilibrium states, the number depending on its parameters. Cell differentiation is then described as a transition from one stable equilibrium point to another, each corresponding to a different cell type.

We pursue an approach consistent with this perception, but introducing several new aspects. The transition from the progenitor to a differentiated state is usually generated by presumed parameter changes in the "core" genetic switch

[a]Electronic mail: schittler@ist.uni-stuttgart.de.

 © 2010 American Institute of Physics

Author complimentary copy. Redistribution subject to AIP license or copyright, see http://cha.aip.org/cha/copyright.jsp

itself, without relation to a biological process.[1,2,6] In our model instead, it is achieved by a preceding switch mechanism, in the following called "preswitch," that in turn influences the state variables in the "fate switch." Stimuli acting on that preswitch part influence the readiness of a cell to differentiate, defining a preliminary phase before final differentiation. A similar concept was previously suggested and modeled in the embryonic stem cell system, where a specific TR determines the differentiation ability of the stem cells.[10]

Furthermore, in order to achieve irreversibility, previous models rely on assuming specific biochemical mechanisms like complex formation or independent processes between transcription factors,[1,2] or they completely neglect activating factors other than autoactivation.[6,7] Although these conditions may be fulfilled in some regulatory circuits, there is no sufficient knowledge about the biochemical details in MSCs to build on such specific assumptions. If the hypothesis of irreversible subsequent cell fate decisions is to hold as the central concept it is proposed,[5] we argue that it has to originate from a more general design principle than some specific cooperative or binding reactions. Our model is set up in a more general way of activating and inhibiting factors all contributing to one functional activity rate, and proposes a preswitch mechanism that generates tristability.

Another crucial point is that asymmetries in parameters between the two mutually inhibiting, unstimulated TRs were so far only considered by a few studies.[2,7] We also study asymmetry (bias) effects on the level of a single cell as well as on population level with stochastic fluctuations: despite the same bias throughout the population, there is not necessarily a homogeneous system behavior in the population. This, in addition, allows to identify and evaluate factors that limit the differentiation success rate in experimental settings.

The aim of our model, functionally describing cell differentiation, is the following. We ask

(1) whether the hypothesized mechanism can generate a system behavior as observed in differentiating cell systems,
(2) to what extent such a minimalistic model can already provide an explanation of the major characteristics of differentiation, and
(3) what insights can be achieved by employing this model for simulations and predictions, such as the differentiation success rate.

This paper is outlined as follows. First, we introduce the biological background and derive the model in Sec. II. Next, we analyze the model with respect to stability, state space, and bifurcation properties in Sec. III. In Sec. IV, we employ our model for simulations on the single cell level as well as on the population level. In Sec. V we conclude with a discussion and some final remarks.

II. MODEL

The biological system under consideration is one of several steps in the differentiation of MSCs: osteochondro progenitor cells that originate from MSCs have already undergone several steps of specialization, remaining bipotent in the sense that they still can differentiate into either osteoblasts or chondrocytes.[11,12]

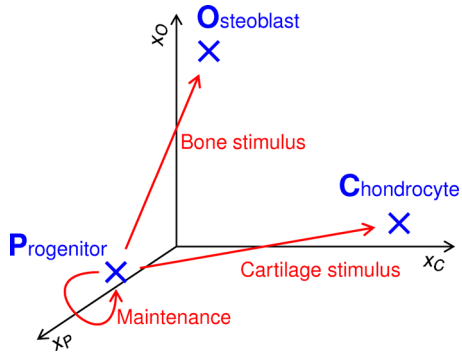

FIG. 1. (Color online) Cell types (×) and transitions between them (→) in differentiation of osteochondro progenitors. Each cell type is recognized by a high level of one of the three TRs (three axes). The possible transitions from the progenitor to a differentiated state take place upon the corresponding stimuli.

This system provides several working assumptions for developing a model: there are three cell types to be captured in terms of stable equilibria, namely, a progenitor (P), an osteogenic (O), and a chondrogenic (C) cell type. Each cell type is recognized by high levels of a characteristic TR, denoted as x_P, x_O, or x_C, respectively, but low levels of the other TRs. This is schematically depicted in Fig. 1 with the axes denoting the TR levels.

It is observed in experiments that there occur certain transitions between the three cell types,[8,12] while others do not. In terms of systems theory, a transition between two cell types means that the system is pushed out of the attractor basin of one stable equilibrium and into the attractor basin of a different stable equilibrium. Let us denote a transition from cell type i to cell type j, $i,j \in \{P,O,C\}$, by $(i \to j)$.

Formulating the biological observations about transitions, there should be only two possible transitions of differentiation, namely,

$$\Delta^{\mathrm{diff}} = \{(P \to O),(P \to C)\}. \tag{1}$$

Other transitions that are not observed in the experimental settings considered here are dedifferentiation

$$\Delta^{\mathrm{de}} = \{(O \to P),(C \to P)\} \tag{2}$$

and transdifferentiation

$$\Delta^{\mathrm{tra}} = \{(O \to C),(C \to O)\}. \tag{3}$$

As depicted in Fig. 1, the MSC thus has three options: to maintain its progenitor state P or to differentiate into either osteoblast O or chondrocyte C.

These observations motivate our concept of a model consisting of two switch parts, each reflecting a different mechanism in the cell system: a preswitch determines whether the cell is able to differentiate at all or remains in the stable progenitor state. Then, the configuration of a fate switch in turn determines into which cell type the cell will differentiate. This concept is in accordance with mechanisms found in the biological system, as will be outlined in the following.

Author complimentary copy. Redistribution subject to AIP license or copyright, see http://cha.aip.org/cha/copyright.jsp

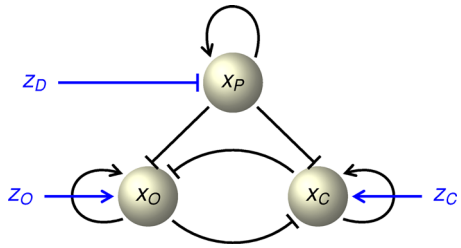

FIG. 2. (Color online) The conceptual model for the OC switch. Positive interactions (activation) are denoted by sharp arrows (→), negative interactions (inhibition) are denoted by stump arrows (⊣). Abbreviations: x_P: progenitor maintenance factor, x_O: osteogenic TR, x_C: chondrogenic TR, z_D: pro-differentiation stimulus, z_O: osteogenic stimulus, z_C: chondrogenic stimulus.

We consider a particular example of two mutually inhibiting key TRs, which determine the cell fate of osteochondro progenitor cells. In the following, we will refer to this pair as the "osteochondro switch" (OC switch): Osx (also Runx2) is established as an osteogenic TR (Ref. 13) and Sox9 as a chondrogenic TR.[11] They inhibit each other's activity via several mechanisms[11,14] and autoregulate their own activity[15–17] as can be found for many TRs.

In addition, we propose a third TR exhibiting a progenitor maintenance role, the preswitch. In our particular example, one candidate would be the cytokine Tweak. It is known to act pro-proliferative, differentiation-inhibiting,[18,19] and thus is a potential regulator of cell fate decisions. In particular, Tweak inhibits osteogenic TRs Runx2, Osx,[20] as well as the chondrogenic TR Sox9.[21] There are various possibilities for autoregulating mechanisms such as autocrine signaling[19] or more extensive signaling loops.

From this collection of qualitative knowledge and requirements, let us now construct a mathematical model. We do not assume that these processes (autoregulation, inhibition) are completely independent of each other, but rather result in an overall activation rate for each component. The system state is represented by the three state variables x_P, x_O, x_C, corresponding to the three respective levels of the progenitor TR, the osteogenic and the chondrogenic TR. Relating to experimental data, these would be (as a rough measure) mRNA levels or (as a more precise measure) transcription factor activities from reporter genes.

Stimuli are assumed to enter the system in the following ways. An unspecific pro-differentiation stimulus will inhibit the progenitor maintenance factor, whereas stimuli acting in the pro-osteogenic or pro-chondrogenic direction enhance the activity level of the lineage-specific TR, respectively. The structure of the OC switch model and stimulus inputs is depicted in Fig. 2. These functional relationships can be summarized in a set of ordinary differential equations as follows:

$$\frac{d}{dt}x_P = \frac{a_P x_P^n + b_P}{m_P + z_D + c_{PP}x_P^n} - k_P x_P, \tag{4}$$

$$\frac{d}{dt}x_O = \frac{a_O x_O^n + b_O + z_O}{m_O + c_{OO}x_O^n + c_{OC}x_C^n + c_{OP}x_P^n} - k_O x_O, \tag{5}$$

TABLE I. Parameter set used for bifurcation analyses and simulations. The parameters are without units.

Parameter	Meaning	Value
n	Hill coefficient	2
a_P	Autoactivation of x_P	0.2
b_P	Basal activity of x_P	0.5
m_P	Inflection point for x_P	10
c_{PP}	Self-inhibition strength of x_P	0.1
k_P	Decay rate of x_P	0.1
a_O, a_C	Autoactivation of x_O, x_C	0.1
b_O, b_C	Basal activity of x_O, x_C	1
m_O, m_C	Inflection point for x_O, x_C	1
c_{OO}, c_{CC}	Self-inhibition strength of x_O, x_C	0.1
c_{OC}, c_{CO}	Mutual inhibition strength of x_O, x_C	0.1
c_{OP}, c_{CP}	Inhibition strength of x_P on x_O, x_C	0.5
k_O, k_C	Decay rates of x_O, x_C	0.1

$$\frac{d}{dt}x_C = \frac{a_C x_C^n + b_C + z_C}{m_C + c_{CC}x_C^n + c_{CO}x_O^n + c_{CP}x_P^n} - k_C x_C, \tag{6}$$

where the coefficient $n \geq 2$, and for $i,j \in \{P,O,C\}$ the state variables x_i are non-negative real numbers, the parameters are real numbers $a_i, b_i, c_{ij}, k_i \in [0,\infty)$, $m_i \in (0,\infty)$. Their meaning and nominal values are given in Table I. The inputs z_i for $i \in \{D,O,C\}$ are each $z_i \in [0, z_i^{\max}]$. Then, z_D corresponds to a lineage-unspecific pro-differentiation stimulus, z_O and z_C to pro-osteogenic and pro-chondrogenic stimuli, respectively. The model could be simplified by reducing the number of parameters, but the paper uses the unreduced equations as the most general representation. Equations (4)–(6) will also be referred to as $d\mathrm{x}/dt = f(x,z)$ for brevity.

Since there is no detailed knowledge of underlying biochemical interactions and the model gives a concept of functional relationships, we introduce several simplifying assumptions. The parameters in the fate switch [Eqs. (5) and (6)] are assigned symmetric values, unless mentioned differently. That means there is no inherent bias of the cell toward one or the other lineage, as long as no lineage-specific stimulus is applied. Second, it is assumed that $n=2$, which is the lowest Hill coefficient producing a sigmoidal shape of the activation term. Qualitative results therefore apply equivalently for higher Hill coefficients $n>2$, arising from more complex reactions.

Third, it is important to note that each input z_D, z_O, z_C is to be seen as "effective" input $z=z([L])$, rather than the amount of actually applied biochemical substance $[L]$ itself. Without knowing the exact function $z([L])$ which depends on further signal processing through pathways, one nevertheless can investigate TR dynamics if solely known, e.g., that $z([L])$ is a monotonically increasing function in $[L]$.

III. ANALYSIS

The aim of analyzing our model is to test whether the proposed model is able to reproduce the cell system properties observed during differentiation. Therefore, we study the stable equilibrium points (Sec. III A) and the transitions in the system (Sec. III B).

Author complimentary copy. Redistribution subject to AIP license or copyright, see http://cha.aip.org/cha/copyright.jsp

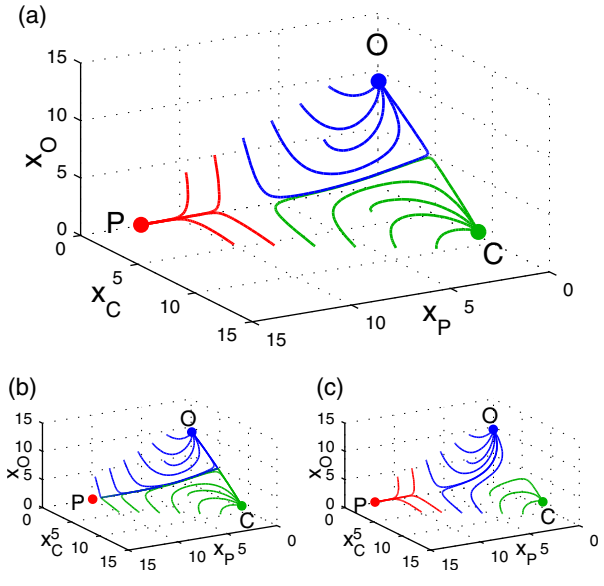

FIG. 3. (Color online) State space, equilibrium points, and exemplary trajectories for (a) $z_D=z_O=0$, (b) $z_D=0.5$, and (c) $z_O=0.5$. The three stable equilibrium points are marked with circles and the corresponding cell type P,O,C. The trajectories visualize the basins of attraction Ω_i. (b) z_D decreases Ω_P and increases Ω_O and Ω_C equally. (c) z_O increases Ω_O and decreases Ω_C without altering Ω_P. Parameters are as in Table I.

A. Stability properties

The cell types of the system are reflected by stable equilibrium points of Eqs. (4)–(6), i.e., solutions $x^*=(x_P^*,x_O^*,x_C^*)^T$ of

$$f(x^*,z)=0 \tag{7}$$

with the Jacobian $Df(x^*,z)$ having eigenvalues λ_k with $\mathrm{Re}(\lambda_k)<0\,\forall k$, with $f(x,z)$ the right-hand side of Eqs. (4)–(6).

As pointed out in Sec. II, biological observations claim the existence of three cell types in the unstimulated case $z=0$, associated with the osteochondro progenitor (recall Fig. 1): the progenitor P (corresponding to the equilibrium state $x^{(P)}$), the osteogenic cell type O (equilibrium state $x^{(O)}$), and the chondrogenic cell type C (equilibrium state $x^{(C)}$). Each equilibrium state $x^{(i)}$, hence cell type $i\in\{P,O,C\}$, is characterized by

$$x_i^{(i)} > x_i^{(j)}\ \forall\, j\neq i, \quad i,j\in\{P,O,C\}, \tag{8}$$

whereas $x_i^{(j)}$ denotes the TR level x_i in the equilibrium state j.

The three cell types are mutually exclusive and are the only ones that should be reflected by our model. Therefore, we claim the existence of exactly three stable solutions to Eq. (7).

The model indeed is able to generate exactly three stable equilibrium points. Figure 3(a) illustrates the three-dimensional state space for an exemplary parameter set as in Table I. Comparing Fig. 3(a) against Fig. 1, one perceives the correct location of stable equilibrium points. As required from biology, the three stable equilibria represent the states P, O, and C, and each satisfies Eq. (8).

Furthermore, each equilibrium point $x^{(i)}$ lies within its attractor basin

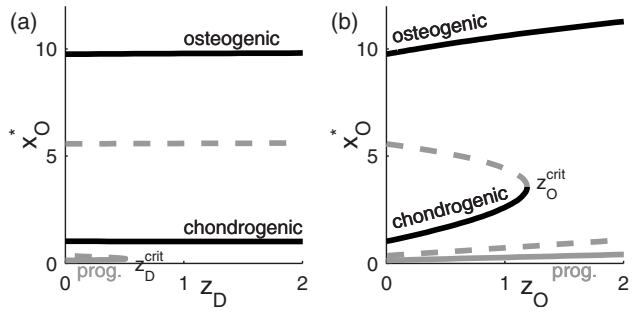

FIG. 4. Bifurcation diagrams for x_O: (a) vs the input z_D and (b) vs the input z_O. Stable equilibrium manifolds are given as solid lines, unstable equilibrium manifolds as dashed lines. The gray solid line corresponds to the P state where x_P is high and thus suppresses x_O generally. The black solid lines correspond to the differentiated states O, C. Parameters are as in Table I. (a) For a sufficiently high input $z_D>z_D^{\mathrm{crit}}$, the system is shifted from a tristable to a bistable regime (Ω_P vanishes) and will either converge to the O or the C stable equilibrium point. After removing the input z_D, the differentiated state is maintained irreversibly. (b) The input z_O can be viewed as acting in a dimension orthogonal to z_D [cf. (a)]. Applying z_O will increase Ω_O, until for $z_O>z_O^{\mathrm{crit}}$ loosing the C state (Ω_C vanishes), which would correspond to transdifferentiation. After removing the input z_O, the state O is maintained irreversibly.

$$\Omega_i := \{\tilde{x}\,|\lim_{t\to\infty} x(t,\tilde{x}) = x^{(i)}\}, \tag{9}$$

whereas $x(t,\tilde{x})$ is the solution of Eqs. (4)–(6) for $x(0)=\tilde{x}$.

The extent of an attractor basin, bordered by separatrices, thereby has an actual meaning in terms of qualitative system properties as well as the biological context: how close the separatrix is to an equilibrium state is one determinant of how robust the system is to fluctuations, e.g., in mRNA production of the respective TR, and to perturbations, e.g., by stimuli. A stimulus input can cause an equilibrium state to vanish and thus induce a transition to another equilibrium. This will be the focus of Sec. III B.

B. Bifurcation properties

Besides the existence of stable equilibrium points, of same interest and importance are the transitions between them (cf. Fig. 1, Sec. II). The differentiation transitions Δ^{diff} [Eq. (1)] should be achievable by transient system inputs, which correspond to stimuli in the biological language. Our model considers three inputs z_D, z_O, and z_C acting on the state variables, as given in Eqs. (4)–(6). Due to symmetrical properties between Eqs. (5) and (6), it is sufficient to investigate only z_O. Equivalent conclusions will then hold for z_C.

The model should allow for the transitions Δ^{diff}, but neither Δ^{tra} nor Δ^{de} [Eqs. (1)–(3)]. Bifurcation analysis [done via CL_MATCONT (Ref. 22)] reveals that, e.g., for the parameter set given in Table I, the model allows exactly the required transitions Δ^{diff}, while excluding Δ^{tra} and Δ^{de} as demanded: the inputs z_D and z_O affect the attractor basins Ω_i and can shift the system from a tristable to a bistable regime, as illustrated in Fig. 4. In this case, coming from the state that is lost upon the input signal, the system will converge to one of the two remaining states. The input z_D decreases Ω_P [Fig. 3(b)] and can switch off the preswitch mechanism for $z_D>z_D^{\mathrm{crit}}$, forcing the system to leave the P state and triggering a differentiation transition Δ^{diff}.

Author complimentary copy. Redistribution subject to AIP license or copyright, see http://cha.aip.org/cha/copyright.jsp

In contrary, the input z_O cannot cause the P state to vanish and thus cannot induce differentiation (Δ^{diff}) by itself. Instead, z_O enlarges Ω_O [Fig. 3(c)]. As can be seen in Fig. 4(b), for a high $z_O > z_O^{\text{crit}}$ the system could switch from state C to state O, which would mean a transdifferentiation Δ^{tra}. Since this behavior is not observed in the considered cell system, the model might give the hint that the effective input z_O, as applied in the experiment, is limited to a $z_O^{\max} < z_O^{\text{crit}}$. Equivalent results hold for z_C.

In realistic parameter sets, there is not necessarily symmetry in parameters between the two lineage-determining TRs x_O and x_C, as we assumed up to this point. This is not only an aspect to be considered, but actually raises more comprehensive investigations on the effects of heterogeneity in parameters. We will show an example scenario in Sec. IV A and consider the asymmetric parameters in a cell population framework in Sec. IV B.

To sum up our results from stability and bifurcation analysis, we have shown that the model we propose is able to capture the fundamental properties of the differentiation process. This means that it can reproduce the observed number of stable equilibrium states as well as the transitions between them.

These system properties not only hold for the exemplary parameter set in Table I, but for a certain range of parameters. For Eq. (4), this is shown analytically in the Appendix. For Eqs. (5) and (6), this was done via extensive bifurcation analysis on the model parameters (not shown here).

IV. DIFFERENTIATION SCENARIOS

After a general analysis from a theoretic viewpoint in Sec. III, in this section we demonstrate how our model can also serve for more descriptive applications to the biological problem. Based on our model, we present two kinds of simulations. First, modeling the behavior of a single cell in Sec. IV A serves to investigate the effects of deterministic or *extrinsic* signals, usually applied on purpose in the form of biochemical stimuli. Second, simulations on a cell population level as in Sec. IV B enable a better understanding of *intrinsic* signals given by heterogeneous or stochastic intracellular properties.

A. Single cell switching

We now demonstrate that our model can reproduce the differentiation process upon extrinsic signals on a single cell scale. In particular, we study stimuli $z_i, i \in \{D, O, C\}$ or combinations of these, potent to induce an osteogenic differentiation transition $(P \to O) \in \Delta^{\text{diff}}$. For simplicity and since the exact functions $z_i([L])$ are unknown, we consider only step function inputs

$$z_i(t) = \begin{cases} Z_i & \text{for } t_i^{(1)} \le t \le t_i^{(2)} \\ 0 & \text{otherwise.} \end{cases} \tag{10}$$

In order to achieve osteogenic differentiation $(P \to O)$, we know from Sec. III B that two goals have to be pursued:

(1) The system has to escape the attractor basin of P.
(2) The system has to enter the attractor basin of O.

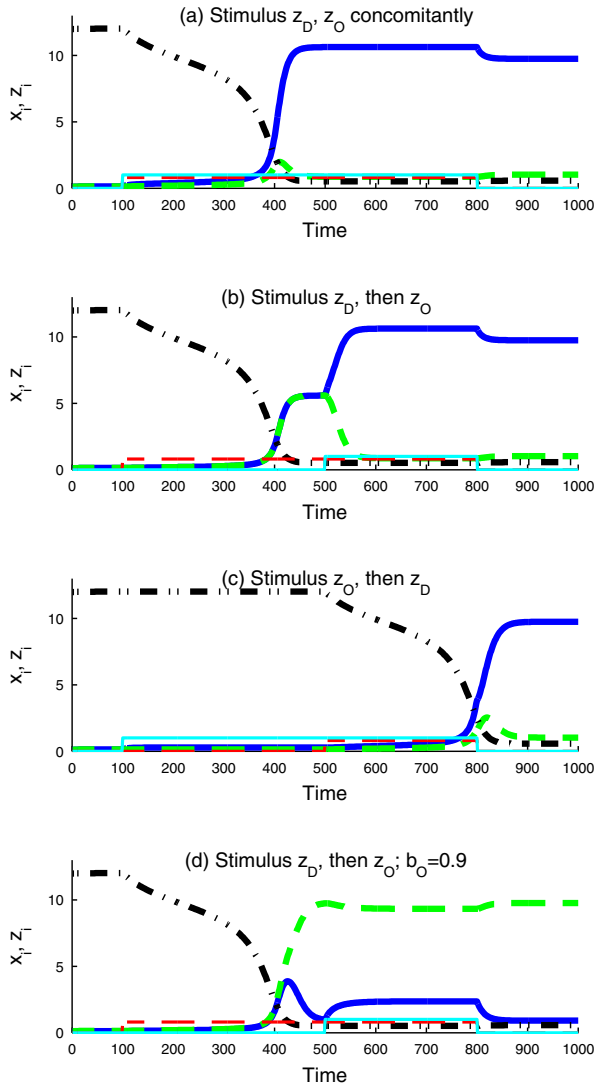

FIG. 5. (Color online) Dynamics of stimulus scenarios (a)–(d) (cf. text). TR dynamics of x_P (black dot-dot-dashed line), x_O (blue solid line), and x_C (green dashed line). Stimulus inputs z_D (red thin dashed line), z_O (cyan thin solid line).

Since z_C does not assist in achieving any of these two goals, we consider combinations of z_D and z_O for the following stimulus scenarios:

(a) z_D, z_O are applied concomitantly: $t_D^{(1)} = t_O^{(1)} = 100$.
(b) z_D is applied first, then z_O: $t_D^{(1)} = 100, t_O^{(1)} = 500$.
(c) z_O is applied first, then z_D: $t_D^{(1)} = 500, t_O^{(1)} = 100$.

In order to investigate the effect of asymmetries in parameters (meaning an intrinsic bias toward one of the two lineages), we furthermore consider the following scenario:

(d) z_D is applied first, then z_O: $t_D^{(1)} = 100, t_O^{(1)} = 500$; but now with $b_O = 0.9 < b_C = 1$, which means a slight intrinsic bias toward chondrogenic lineage; remaining parameters as in Table I.

For all scenarios, we set $Z_D = 0.8 > z_D^{\text{crit}}, Z_O = 1 < z_O^{\text{crit}}$, $t_D^{(2)} = t_O^{(2)} = 800$ always, parameters as in Table I.

The outcomes of scenarios (a)–(d) are depicted in Fig. 5. The observations will be discussed in the following.

Author complimentary copy. Redistribution subject to AIP license or copyright, see http://cha.aip.org/cha/copyright.jsp

In scenario (a), the concomitant application of z_D and z_O induces escape from the P state and attraction to the O state [Fig. 5(a)]. This is also what one expects from systems analysis (Sec. III).

In scenario (b), first z_D causes x_P to decrease, thus both x_O and x_C increase to an equal value [Fig. 5(b)]; not until z_O is added, x_O fully increases and x_C again decreases to a low value, corresponding to state O. This can be understood by recalling the system properties: when only first z_D is applied, it temporarily shifts the system from a tristable to a bistable regime [cf. Fig. 4(a)], causing the system to escape the P state. Since this scenario assumes symmetry of parameters in Eqs. (5) and (6), and in initial values of x_O and x_C as well, the system state will preliminary remain at a point on the separatrix between the two differentiated stable states (cf. Fig. 3). Then, adding z_O pushes the system finally into the O attractor basin Ω_O.

It is of course important to note that any asymmetries in parameters, initial values, or stochastic fluctuations could cause a deviation from the unstable state and thus attraction to O or C state, depending on the particular deviation. As a consequence, the eventual system fate completely eludes controlled guidance. In order to avoid this case, a reasonable guideline would be to never apply a stimulus z_D alone before the additional application of the lineage-specific stimulus z_O.

In scenario (c), the two stimuli are applied in the opposite order, thus avoiding the problem just discussed. As seen in Fig. 5(c), first applying z_O slightly increases x_O, but cannot cause the P state to vanish [cf. Fig. 4(b)]. In terms of Fig. 3, this means that the P state is shifted slightly toward O, but the system is still trapped in Ω_P. Not until z_D is added, the tristable regime is left to bistability, where due to the effect of z_O the system enters Ω_O. In this scenario, the differentiation process is completely under control. (We will see in Sec. IV B that further limitations on this control might be imposed when considering stochastic effects.)

The so far presumed symmetric parameters are a special case, but are not the case in general. In scenario (d), the value of b_O (the basal activity of the osteogenic TR) is not set equally to b_C (the basal activity of the chondrogenic TR), but to a smaller value: $b_O=0.9=0.9b_C$. As seen in Fig. 5(d), upon applying z_D and loosing the P state, the system falls into Ω_C and thus x_C increases to $x_C>x_O$. The application of z_O cannot reattract the system to Ω_O any more: the system is already trapped too deeply in Ω_C and, since in the scenario z_O is limited to $z_O^{\max}<z_O^{\text{crit}}$, there exists a certain time point ($t\leq t_O^{(1)}=500$ here) from which on the input z_O is not sufficient any more for the system to escape Ω_C. This again confirms that asymmetries in parameters can play a crucial role, especially if an unspecific stimulus z_D is to exhibit its effect before the lineage-specific stimulus z_O, as in scenario (b).

To sum up the observed dynamics in the simulation scenarios, we can restrict stimulus combinations for successful osteogenic differentiation by the following requirements:

(1) There has to be a sufficiently large $z_D>z_D^{\text{crit}}$ [cf. Fig. 4(a)] in order to leave Ω_P.
(2) As soon as the attractor basin of P is left, and any deviation from the separatrix occurs, e.g., due to initial state values asymmetric between x_O and x_C, the system will converge to O or C. There has to be an osteogenic stimulus z_O in order to safely guide the system to Ω_O.
(3) Asymmetries in parameters or initial values may impose a bias toward one or the other lineage; in case of a bias toward C, z_O has to be sufficiently large in order to overcome this bias and instead guide the system into Ω_O.
(4) The inputs have to be present long enough and at the crucial time points: z_D has to act sufficiently long for x_P to leave Ω_P in order to achieve irreversible escape. z_O has to act sufficiently long to drive the system into Ω_O.

As seen, not only the combination and amount of stimuli are crucial, but also the sequence of what times they become effective.

None of the two inputs z_D, z_O alone is sufficient to execute a transition guided toward one specific cell type O or C. So in order to steer the system on purpose toward the desired (say, osteogenic O) state, a combination of both inputs is necessary. Biologically, combining the two inputs in any desirable way requires that z_D, z_O could be achieved by biochemically distinct substances and pathways. Indeed, classical osteogenic differentiation medium consists of several biochemical substances (e.g., dexamethasone, ascorbic acid, and β-glycerophosphate[23]) with probably different analog to z_D or z_O. Our model can serve to apply hypothetical stimulus combinations and sequences and compare the resulting outcomes.

B. Cell population effects

The differentiation scenarios examined so far were all based on a deterministic single cell model, such that the system response to some input signal was precisely as predicted by the bifurcation analysis. But, as already indicated in Sec. III B, under realistic circumstances the states are subject to stochastic fluctuations.[24] This section will examine these intrinsic signals: they escape the control via experimental manipulations, contrary to the extrinsic signals covered in Sec. IV A, and thus can impose limitations on the differentiation success rate.

To account for stochastic fluctuations during the transcription process,[25] i.e., on the activation rates, the model equations are extended to a set of stochastic differential equations[26,27] with independent white noise W_i, $i\in\{P,O,C\}$,

$$dx_P=-k_Px_Pdt+\frac{a_Px_P^n+b_P}{m_P+z_D+c_{PP}x_P^n}(dt+\sigma dW_P), \tag{11}$$

$$dx_O=-k_Ox_Odt+\frac{a_Ox_O^n+b_O+z_O}{m_O+c_{OO}x_O^n+c_{OC}x_C^n+c_{OP}x_P^n}(dt+\sigma dW_O), \tag{12}$$

Author complimentary copy. Redistribution subject to AIP license or copyright, see http://cha.aip.org/cha/copyright.jsp

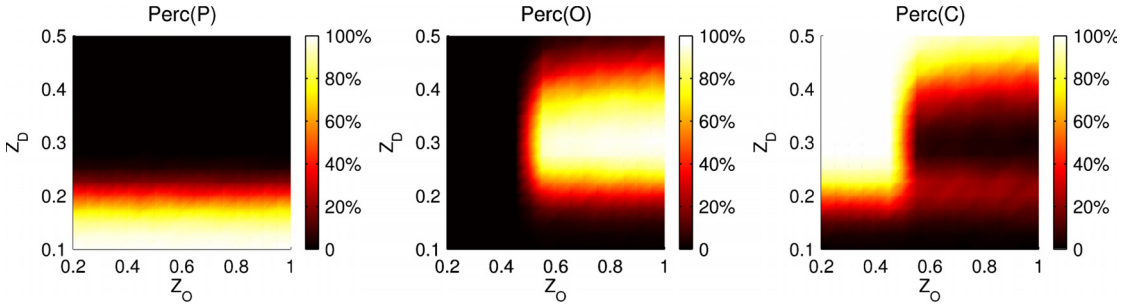

FIG. 6. (Color online) Perc(P), Perc(O), and Perc(C) after stimuli were applied with $z_D(t)=Z_D$ for $t\in[100,800]$, $z_O(t)=Z_O$ for $t\in[400,800]$ (cf. text for details). Perc(P) is only determined by Z_D. Perc(O) has its maximum for intermediate Z_D and high Z_O, decreasing again for high Z_D. Perc(C) has its maximum for high Z_D, but low Z_O; also, it peaks for intermediate and high Z_D regardless of Z_O.

$$dx_C = -k_C x_C dt + \frac{a_C x_C^n + b_C + z_C}{m_C + c_{CC}x_C^n + c_{CO}x_O^n + c_{CP}x_P^n}(dt + \sigma dW_C), \tag{13}$$

with σ the standard deviation, which was solved via a Euler–Maruyama scheme.[28]

As in Eq. (10), stimuli are applied as step function inputs, again $t_D^{(2)}=t_O^{(2)}=800$. For noise $\sigma=0.4$ is chosen such that the state variables x_i experience a coefficient of variation of about 0.07, which is a level of noise that is found reasonable in similar systems.[25]

We then investigate the effect of different levels of Z_D and Z_O on the percentage of cells that are finally in state P, O, or C,

$$\text{Perc}(i) := 100\% \cdot \text{Probability}(x \in \Omega_i), \quad i \in \{P,O,C\}. \tag{14}$$

The probability was approximated by using N simulations of x as in Eqs. (11)–(13).

To investigate how capable a lineage-specific stimulus z_O is to guide the system toward O, a strong inherent bias toward the competing state C was created by setting $b_O=0.5<b_C=1$, all other parameters as in Table I. Simulations were done for a population of $N=1000$ cells for $t\in[0,1000]$. Stimuli were applied $z_D(t)=Z_D$ for $t\in[t_D^{(1)},t_D^{(2)}]=[100,800]$ and $z_D(t)=0$ otherwise, $z_O(t)=Z_O$ for $t\in[t_O^{(1)},t_O^{(2)}]=[400,800]$ and $z_O(t)=0$ otherwise. The percentages Perc(i) were determined by how many trajectories remained in Ω_i under deterministic conditions.

In Fig. 6 it can be seen that the percentages of cells depend on the amounts of stimuli Z_D and Z_O in a highly nonlinear way. Perc(P) is only determined by Z_D, as expected. It is almost 100% below some threshold for Z_D, meaning that the stochasticity is not sufficient to induce differentiation on its own, and minimal 0 above another threshold, although this threshold still fulfills $Z_D<z_D^{\text{crit}}$, i.e., stochasticity is sufficient to push each cell over the limit point z_D^{crit} at some time instance $t\in[100,800]$.

Perc(O) has its maximum for intermediate Z_D and high Z_O, but decreases again for high Z_D. This happens because if $z_D(t)$ is high, many cells leave Ω_P before $z_O(t)=Z_O$ becomes effective, therefore having a bias to Ω_C (due to the parameter $b_O=0.5<b_C=1$).

Perc(C) has the maximum value of 100% for high Z_D, but low Z_O; besides, it has two peaks for low and high Z_D regardless of Z_O. The first peak for low Z_D occurs because for a low $z_D(t)$, also $z_O(t)$ cannot exhibit its full effect: the differentiation process is mainly initiated by stochastic fluctuations rather than the deterministic parameters. The second peak for high Z_D originates from the same effect responsible for the decrease of Perc(O) for high Z_D, namely, because many cells leave Ω_P and enter Ω_C before Z_O gets effective.

After comparing the amounts of stimuli, we also considered the effect of their timing. Regarding the duration $(t_D^{(2)}-t_D^{(1)})$ where $z_D(t)=Z_D$, it was observed that increasing $(t_D^{(2)}-t_D^{(1)})$ has qualitatively the same effect as increasing Z_D (proven by equivalent analysis). For the osteogenic stimulus z_O, the dependency is less obvious: an input $z_O(t)=Z_O$ enlarges Ω_O, but does not alter Ω_P (cf. Sec. III B). Thus, it cannot exhibit its effect as long as $z_D(t)=0$. Therefore, we investigated the change of percentages Perc(i) upon $(t_O^{(1)}-t_D^{(1)})$, i.e., the delay between effective inputs Z_D and Z_O. Figure 7 depicts the results exemplarily for $Z_D=0.4$, $Z_O=0.55$, remaining values as before. Clearly, the timing of z_O after z_D plays a crucial role for the differentiation success rate, in this case measured in the percentage of osteogenic cells Perc(O).

Summing up, our model demonstrates that stochasticity on the one hand can induce differentiation although z_D is below the (deterministic) threshold z_D^{crit}, but on the other hand can also limit the differentiation success rate. The studies here indicate that a limited differentiation success rate may be due to a pro-differentiation stimulus z_D that lies below the threshold for differentiation under deterministic circumstances.

V. DISCUSSION

We have developed a model of cell differentiation, in particular, of the osteochondro progenitor cell, based on in-

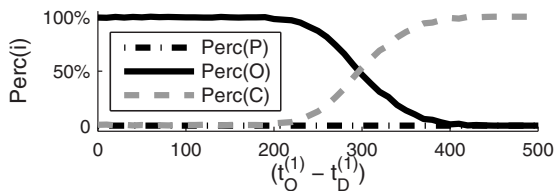

FIG. 7. Perc(P), Perc(O), and Perc(C) vs delay $(t_O^{(1)}-t_D^{(1)})$ of stimulus z_O (cf. text for details). There is a clear dependency of Perc(O) and Perc(C) [but not of Perc(P)] on how late z_O is applied.

Author complimentary copy. Redistribution subject to AIP license or copyright, see http://cha.aip.org/cha/copyright.jsp

teractions between key TRs. As we have shown, the model is able to reproduce the biological observations: the existence of three stable equilibrium states (cell types), and the two transitions when the cell leaves the progenitor state and adopts osteogenic (bone) or chondrogenic (cartilage) lineage.

Our model proceeds in the established manner of minimal gene regulatory network models.[1,2] The particular example of such a genetic switch considered here comprises the well-known motif of two mutually inhibiting TRs. But it differs from previous models of bistable switches where loss of the progenitor state was achieved by changing parameters, and based on specific assumptions on cooperativity, complex formations, or independency of processes. The model presented in this work instead contains an additional TR that is responsible for maintaining the progenitor state as indicated by experimental observations, incorporating a concept similarly reported in the embryonic stem cell system.[10] This work shows that models for cell fate switches need to have three stable equilibrium states, and that this can be achieved reliably via a generic model of two separated decisions: triggering differentiation by a preswitch and fate determination by a fate switch.

In this way, the model suits the framework of binary cell fate decisions executed by subsequent switch modules:[5] the process in the preswitch can be seen as the result of a genetic switching at an earlier step, which in turn may again be one of mutually inhibiting TRs. Alternatively, our model may serve as a module to be incorporated within a set of nonhierarchical cell fate decisions.[6,7] With one such module provided by our model, it will be the task for future work to implement and interconnect to further modules, such as for the cell fate decision between adipogenic and osteochondro progenitor lineages. Such modeling frameworks, and their comparison, have the potential to contribute to a comprehensive understanding of MSC differentiation down to fully matured bone, cartilage, fat cells, and other cell types.

Our main message is that the proposed mechanism, although based on very coarse and qualitative knowledge about functional relations, can give an explanation on how differentiation might function. What is more, it can also unravel how differentiation might (or might not) be guided into a specific direction. For this purpose, we analyzed the multiinput response to stimuli applied in various combinations and sequences. Bifurcation analysis and simulations on single cell scale reveal that not only the amount of stimuli but also their combination and timing may play a crucial role for the eventually adopted cell fate. To obtain more detailed, quantitative predictions about stimulus effects, additional modeling of the pathways from applied substances to effective inputs on TRs is required.

Furthermore, we extended our model to the level of cell populations with stochastic single cell dynamics to study the effect of stochasticity, stimulus amounts, combinations, and sequences on the differentiation outcome. We were able to show that stochastic effects might induce differentiation events already below the (deterministic) threshold and limit the differentiation success rate. The proposed model can serve to indicate potential factors, such as stimulus timing, to suggest experimental protocols and improve the differentiation success rate. Due to its coarse and functional character, it is especially suited for such fundamental investigations. Our model may provide an explanation why MSC differentiation requires a combination of several stimuli associated with different effects, and why the amount and sequence of stimuli might be relevant for the eventual differentiation success rate.

ACKNOWLEDGMENTS

The authors would like to thank for financial support the German Research Foundation (DFG) within the Cluster of Excellence in Simulation Technology (Grant No. EXC 310/1) at the University of Stuttgart and from the German Federal Ministry of Education and Research (BMBF) within the SysTec program (Grant No. 0315506A) and the FORSYS-Partner program (Grant No. 0315280A). D.S. acknowledges the financial support from The MathWorks Foundation of Science and Engineering.

APPENDIX: SUFFICIENT CONDITIONS PRESWITCH

Equation (4) can be rewritten in a dimensionless form for $n=2$ as

$$\frac{d}{d\tau}x = \frac{\alpha x^2 + 1}{1 + \zeta_D + \gamma x^2} - x \tag{A1}$$

by substituting $x=(m_P k_P/b_P)x_P$, $\tau=k_P t$, $\alpha=a_P b_P/m_P^2 k_P^2$, $\gamma=c_{PP}b_P^2/m_P^3 k_P^2$, $\zeta_D=z_D/b_P$.

(I) First, we derive the necessary and sufficient conditions for Eq. (A1), $z_D=0$, having exactly two (non-negative) stable equilibrium states, which is equivalent to the existence of exactly three solutions x to

$$\frac{d}{d\tau}x = \frac{\alpha x^2 + 1}{1 + \gamma x^2} - x \stackrel{!}{=} 0. \tag{A2}$$

All solutions satisfy $x \geq 0$ since the parameters $\alpha, \gamma > 0$. Equation (A2) is equivalent to

$$p(x) := \gamma x^3 - \alpha x^2 + x - 1 \stackrel{!}{=} 0, \tag{A3}$$

which has exactly three solutions if and only if the equation

$$\frac{\partial}{\partial x}p(x) = 3\gamma x^2 - 2\alpha x + 1 = 0 \tag{A4}$$

has two solutions (i) $x_{1,2}=\alpha \pm \sqrt{\alpha^2 - 3\gamma}/3\gamma \geq 0$ and (ii) $p(x_1)<0, p(x_2)>0$. It holds that

$$\begin{aligned} &\text{(i)} \Leftrightarrow \alpha > \sqrt{3\gamma}, \\ &\text{(ii)} \Leftrightarrow \left(0 < \alpha \leq \tfrac{1}{4} \wedge 0 < \gamma < (s_1 + s_2)\right) \\ &\qquad \vee \left(\tfrac{1}{4} < \alpha \leq \tfrac{1}{3} \wedge (s_1 - s_2) < \gamma < (s_1 + s_2)\right), \end{aligned} \tag{A5}$$

whereas $s_1=\frac{1}{27}(-2+9\alpha)$ and $s_2=\frac{2}{27}\sqrt{1-9\alpha+27\alpha^2-27\alpha^3}$.

Thus, for parameters α, γ satisfying Eq. (A5), it is guaranteed that x_P can have an "on" and an "off" state.

(II) Second, we proof that there always exists a finite stimulus $\zeta := \zeta_D^{\text{crit}} > 0$ such that there is exactly one stable equilibrium solution x to

Author complimentary copy. Redistribution subject to AIP license or copyright, see http://cha.aip.org/cha/copyright.jsp

$$\frac{d}{d\tau}x = \frac{\alpha x^2 + 1}{1 + \zeta + \gamma x^2} - x \stackrel{!}{=} 0. \tag{A6}$$

This is equivalent to

$$q(x) := \gamma x^3 - \alpha x^2 + (\zeta + 1)x - 1 \stackrel{!}{=} 0, \tag{A7}$$

which in turn has exactly one solution if

$$\frac{\partial}{\partial x}q(x) = 3\gamma x^2 - 2\alpha x + (\zeta + 1) = 0 \tag{A8}$$

has at most one solution.

It can be shown that this holds if and only if $\alpha^2 < 3\gamma(\zeta+1)$, i.e., if and only if $\zeta > \alpha^2/3\gamma - 1$. Since from (I) one knows $1 < \alpha^2/3\gamma < \infty$, it is $0 < \zeta$ and there always exists a $\zeta^{\text{crit}} < \infty$ such that there is exactly one stable equilibrium solution.

Thus, there is always a stimulus ζ_D that can irreversibly switch off x_P.

[1] S. Huang, Y.-P. Guo, G. May, and T. Enver, "Bifurcation dynamics in lineage-commitment in bipotent progenitor cells," Dev. Biol. **305**, 695 (2007).

[2] I. Roeder and I. Glauche, "Towards an understanding of lineage specification in hematopoietic stem cells: A mathematical model for the interaction of transcription factors GATA-1 and PU.1," J. Theor. Biol. **241**, 852 (2006).

[3] S. Palani and C. A. Sarkar, "Integrating extrinsic and intrinsic cues into a minimal model of lineage commitment for hematopoietic progenitors," PLOS Comput. Biol. **5**, e1000518 (2009).

[4] V. Chickarmane, T. Enver, and C. Peterson, "Computational modeling of the hematopoietic erythroid-myeloid switch reveals insights into cooperativity, priming, and irreversibility," PLOS Comput. Biol. **5**, e1000268 (2009).

[5] D. V. Foster, J. G. Foster, S. Huang, and S. A. Kauffman, "A model of sequential branching in hierarchical cell fate determination," J. Theor. Biol. **260**, 589 (2009).

[6] O. Cinquin and J. Demongeot, "High-dimensional switches and the modelling of cellular differentiation," J. Theor. Biol. **233**, 391 (2005).

[7] B. D. MacArthur, C. P. Please, and R. O. C. Oreffo, "Stochasticity and the molecular mechanisms of induced pluripotency," PLoS ONE **3**, e3086 (2008).

[8] D. Baksh, L. Song, and R. S. Tuan, "Adult mesenchymal stem cells: Characterization, differentiation, and application in cell and gene therapy," J. Cell. Mol. Med. **8**, 301 (2004).

[9] T. S. Gardner, C. R. Cantor, and J. J. Collins, "Construction of a genetic toggle switch in Escherichia coli," Nature (London) **403**, 339 (2000).

[10] I. Glauche, M. Herberg, and I. Roeder, "Nanog variability and pluripotency regulation of embryonic stem cells—insights from a mathematical model analysis," PLoS ONE **5**, e11238 (2010).

[11] G. Zhou, Q. Zheng, F. Engin, E. Munivez, Y. Chen, E. Sebald, D. Krakow, and B. Lee, "Dominance of SOX9 function over RUNX2 during skeletogenesis," Proc. Natl. Acad. Sci. U.S.A. **103**, 19004 (2006).

[12] T. J. Heino and T. A. Hentunen, "Differentiation of osteoblasts and osteocytes from mesenchymal stem cells," Curr. Stem Cell Res. Ther. **3**, 131 (2008).

[13] H.-M. Ryoo, M.-H. Lee, and Y.-J. Kim, "Critical molecular switches involved in BMP-2-induced osteogenic differentiation of mesenchymal cells," Gene **366**, 51 (2006).

[14] K. Nakashima and B. de Crombrugghe, "Transcriptional mechanisms in osteoblast differentiation and bone formation," Trends Genet. **19**, 458 (2003).

[15] M. Phimphilai, Z. Zhao, H. Boules, H. Roca, and R. T. Franceschi, "BMP signaling is required for RUNX2-dependent induction of the osteoblast phenotype," J. Bone Miner. Res. **21**, 637 (2006).

[16] H. Drissi, Q. Luc, R. Shakoori, S. C. de Sousa Lopes, J.-Y. Choi, A. Terry, M. Hu, S. Jones, J. C. Neil, J. B. Lian, J. L. Stein, A. J. van Wijnen, and G. S. Stein, "Transcriptional autoregulation of the bone related CBFA1/RUNX2 gene," J. Cell. Physiol. **184**, 341 (2000).

[17] D. Kumar and A. B. Lassar, "The transcriptional activity of Sox9 in chondrocytes is regulated by RhoA signaling and actin polimerization," Mol. Cell. Biol. **29**, 4262 (2009).

[18] M. Girgenrath, S. Weng, C. A. Kostek, B. Browning, M. Wang, S. A. Brown, J. A. Winkles, J. S. Michaelson, N. Allaire, P. Schneider, M. L. Scott, Y.-M. Hsu, H. Yagita, R. A. Flavell, J. B. Miller, L. C. Burkly, and T. S. Zheng, "TWEAK, via its receptor Fn14, is a novel regulator of mesenchymal progenitor cells and skeletal muscle regeneration," EMBO J. **25**, 5826 (2006).

[19] J. A. Winkles, N. L. Tran, S. A. N. Brown, N. Stains, H. E. Cunliffe, and M. E. Berens, "Role of Tweak and Fn14 in tumor biology," Front. Biosci. **12**, 2761 (2007).

[20] C. Vincent, D. M. Findlay, K. J. Welldon, A. R. Wijenayaka, T. S. Zheng, D. R. Haynes, N. L. Fazzalari, A. Evdokiou, and G. J. Atkins, "Pro-inflammatory cytokines TNF-related weak inducer of apoptosis (TWEAK) and TNFα induce the mitogen-activated protein kinase (MAPK)-dependent expression of sclerostin in human osteoblasts," J. Bone Miner. Res. **24**, 1434 (2009).

[21] H. Huh, Y.-J. Lee, J.-H. Kim, M.-H. Kong, K.-Y. Song, and G. Choi, "The effects of Tweak, Fn14, and TGF-beta1 on degeneration of human intervertebral disc," J. Kor. Neuro. Soc. **47**, 30 (2010).

[22] A. Dhooge, W. Govaerts, and Y. A. Kuznetsov, "MATCONT: A MATLAB package for numerical bifurcation analysis of ODEs," ACM Trans. Math. Softw. **29**, 141 (2003).

[23] C. Shui, T. C. Spelsberg, B. L. Riggs, and S. Khosla, "Changes in Runx2/Cbfa1 expression and activity during osteoblastic differentiation of human bone marrow stromal cells," J. Bone Miner. Res. **18**, 213 (2003).

[24] A. Raj and A. van Oudenaarden, "Nature, nurture, or chance: Stochastic gene expression and its consequences," Cell **135**, 216 (2008).

[25] J. M. Pedraza and J. Paulsson, "Effects of molecular memory and bursting on fluctuations in gene expression," Science **319**, 339 (2008).

[26] D. T. Gillespie, "The chemical Langevin equation," J. Chem. Phys. **113**, 297 (2000).

[27] D. J. Wilkinson, *Stochastic Modelling for Systems Biology* (Chapman and Hall, London/CRC, Boca Raton, FL, 2006).

[28] D. Higham, "An algorithmic introduction to numerical simulation of stochastic differential equations," SIAM (Soc. Ind. Appl. Math.) J. Numer. Anal. **43**, 525 (2001).

Author complimentary copy. Redistribution subject to AIP license or copyright, see http://cha.aip.org/cha/copyright.jsp